Journal of the European Ceramic Society 21 (2001) 2369–2376

www.elsevier.com/locate/jeurceramsoc

Shape, size and composition of mullite nanocrystals from a rapidly sintered kaolin

O. Castelein [a], R. Guinebretière [b], J.P. Bonnet [a], P. Blanchart [a,*]

[a] *GEMH, Ecole Nat. Sup. de Ceramique Indus. ENSCI, 48–73 Avenue Albert Thomas, 87605 Limoges, France*
[b] *SPCTS, CNRS, Limoges, France*

Received 14 September 2000; accepted 16 December 2000

Abstract

The characteristics of mullite crystallites from a kaolin raw material were determined at the early stage of crystallisation by X-ray diffractometry. The equipment was a Debye–Scherrer system equipped with a curved position sensitive detector. We measured the size and shape of mullite crystallites in relation to the temperature (1100–1150°C) and the temperature rate (3–20°C/min). In particular, a temperature rate influence was found on crystallites anisotropy. This result was satisfactorily correlated with TEM observations of sintered materials. The mullite cells constants were also measured, they vary significantly with sintering conditions. Cell constants were correlated with mullite stœchiometry using the Cameron relationship. Results indicated a narrow composition domain (62–65% Al_2O_3) for all thermal cycles. In each case, the orthorhombic phase was identified, in spite of the low temperature range studied and the relatively high alumina content.

Keywords: Kaolin; Mullite; Sintering; X-ray methods

1. Introduction

A major trend affecting the ceramic industry is the use of fast firing, as in the case of floor and wall tiles, which are fired in the range 1050–1250°C, using temperature rates up to 60°C/min. Fast firing induces a large change of thermal transformations of raw materials and their mixtures.

Kaolin raw materials are often used in the manufacture of ceramics. They are complex mixtures of more or less ordered kaolinite, a mica group mineral and quartz. Minor quantities of other minerals may be present. The understanding of raw material thermal comportment requires knowledge of the mineral individual behaviours and also their mutual interactions at high temperature. But numerous problems raise from the large range of mineral properties and from the discrepancy between behaviour of natural mineral mixtures and that of reference mineral mixtures.[1]

Mullite crystallisation is a common phenomenon involved in the thermal transformation of clay minerals. The quantity and development of this phase influence the sintering mechanisms, but mullite formation depends on the raw material type and is modified by the firing process.

To find out more about kaolin fast sintering, we chose to study the mullite crystallisation from a particular kaolin raw material containing kaolinite, a muscovite mica phase and quartz. The basic idea is to observe the thermal transformations of a simple as possible raw material, in the absence of a liquid phase, i.e. at the early stage of mullite nucleation and growth. For the kaolin studied, we verified the absence of any liquid phase by an ultrasonic method,[2,3] as the apparent Young's modulus of a ceramic sample being strongly sensitive to microstructural changes. Although the eutectic temperature of the hypothetically homogeneous material is at 1140°C,[4] results revealed rather a 1190°C temperature.[2]

Mullite formation and characteristics were studied in relation to a temperature of 1100 and 1150°C, when the material densification is rapid. We used 3°C/min and 20°C/min temperature rates, which are equivalent to traditional or more accelerated firing cycles.

* Corresponding author. Tel.: +33-5-55-45-22-22; fax: +33-5-55-79-09-98.
E-mail address: p.blanchart@ensci.fr (P. Blanchart).

0955-2219/01/$ - see front matter
PII: S0955-2219(01)00211-4

2. Materials and methods

The chosen raw material (Bio, from Echassière, France)[5] is a selected kaolin containing a reduced quantity of mineral impurities. Table 1 reports the chemical analysis. From X-ray diffraction and chemical analysis by ICP, the mineralogical composition was determined (79±2% kaolinite, 17±2% muscovite mica and 4±1% quartz). The cristallinity degree of the kaolinite phase[6] is high (Hinckley index 0.98), compared to that of the well known kaolinite reference mineral Kga1[7] (Hinckley index 1.03). For the muscovite mineral, the peak heights and broadening of the (00l) X-ray reflections are very similar to those of a typical and well crystallised muscovite.[2]

Besides these minerals, the iron major impurity was studied by Mössbauer spectroscopy.[2] About 50% of the total Fe amount was located as a structural element in clay minerals, mainly in the muscovite phase. The remainder was observed in Fe hydroxide phases, which transforms progressively to hematite above about 500°C.

A preliminary granulometry analysis of minerals, by SEM, revealed small kaolinite grains (~2 μm) around, obviously very different and larger, muscovite grains (~5–10 μm). The relatively larger quartz grains (~10–20 μm) and its low content (4%) will ensure that material characterisation can be significantly attributed to the clay minerals.

X-ray diffractometry was carried out using a Debye–Scherrer system equipped with a curved position sensitive detector (CPS 120 Inel). The Cu K_{α_1} X-ray line was selected using a bent quartz crystal monochromator. The spatial position of the flat sample holder was precisely adjusted to obtain a match between the diffractometer axis and the specimen surface.[8] To avoid a textural effect, samples were continually rotated around their normal axis during experiments.

All measurements were performed in a reflection mode and the incident angle of the beam onto the sample surface was fixed at 5°. This value allows the observation of diffraction lines in the low angular range, but increases the instrumental broadening effect.[9]

For all experiments, the signal/noise ratio was improved using a 14-h data collection system.

The direct observation of crystallite sizes was performed by transmission electron microscopy with a 200 kV Jeol 2010. A drop of powder suspension was deposited onto an amorphous carbon film on a copper grid.

Table 1
Chemical composition of the Bio kaolin

Wt.%	Bio
SiO_2	47.10
Al_2O_3	36.70
Fe_2O_3	1.16
TiO_2	0.07
CaO	0.11
MgO	0.21
Na_2O	0.11
K_2O	2.17
Li_2O	0.11
P_2O_5	–
Loss on ignition	12.26

3. Results

An example of the X-ray pattern is shown in Fig. 1a, for Bio material fired at 1100°C, 3°C/min. The only crystalline phases are residual quartz, and the newly formed mullite. Fig. 1b shows the most representative reflections, (210) and (120) of mullite, for two different thermal cycles, 1100°C at 3°C/min and 1150°C at 20°C/min. A comparison was also made with a sample maintained for 12 h at 1100°C.

The micro-structural characteristics of the studied sample were determined by line profile analysis of the diffraction peaks. The profile refinements were realised using Peakoc software[9] and the instrumental line profile contribution was evaluated using the NIST standard sample LaB_6 (SRM 660).

Previous publications,[9,10] described the low influence of transparency and divergence effect in such diffraction geometry. Consequently, the instrumental line profile effect is close to a symmetric one and can be fitted by a Voigt function. The pure sample broadening effects were obtained using the Voigt method introduced by J.I. Langford[11] and developed by D. Balzar,[12] assuming that both size and micro-strains induce a Voigtian effect.

In Fig. 2, the integral breadth of diffraction lines from the LaB_6 standard material is compared with that of the mullite of Bio against (°2θ). The instrumental resolution function was obtained using a quadratic form on (°2θ) by a least-square fit of data. For mullite, the diffraction integral breadths are much wider than those from the instrumental resolution function. This indicates an intrinsic broadening effect from the studied material. Furthermore, the scattering of the breadth values clearly indicates the anisotropic character of the broadening effect. Breadth variations are much greater than the measurement uncertainties, which are about 0.01°2θ.

The separation of the size and micro-strain effects was carried out using Williamson–Hall plots.[13] A typical result is presented in Fig. 3 for the sample fired at 1100°C, 3°C/min. For the two perpendicular directions, (hh0) and (00l), the plotted line slopes are very low, indicating that the main broadening effect is the size effect. The anisotropy of the broadening effect is clearly shown. β^* values of the (hh0) diffraction lines are two or three time larger than that of the (00l) peaks. In Fig. 3, the non-zero intercept effect of the β^* line for the (hh0)

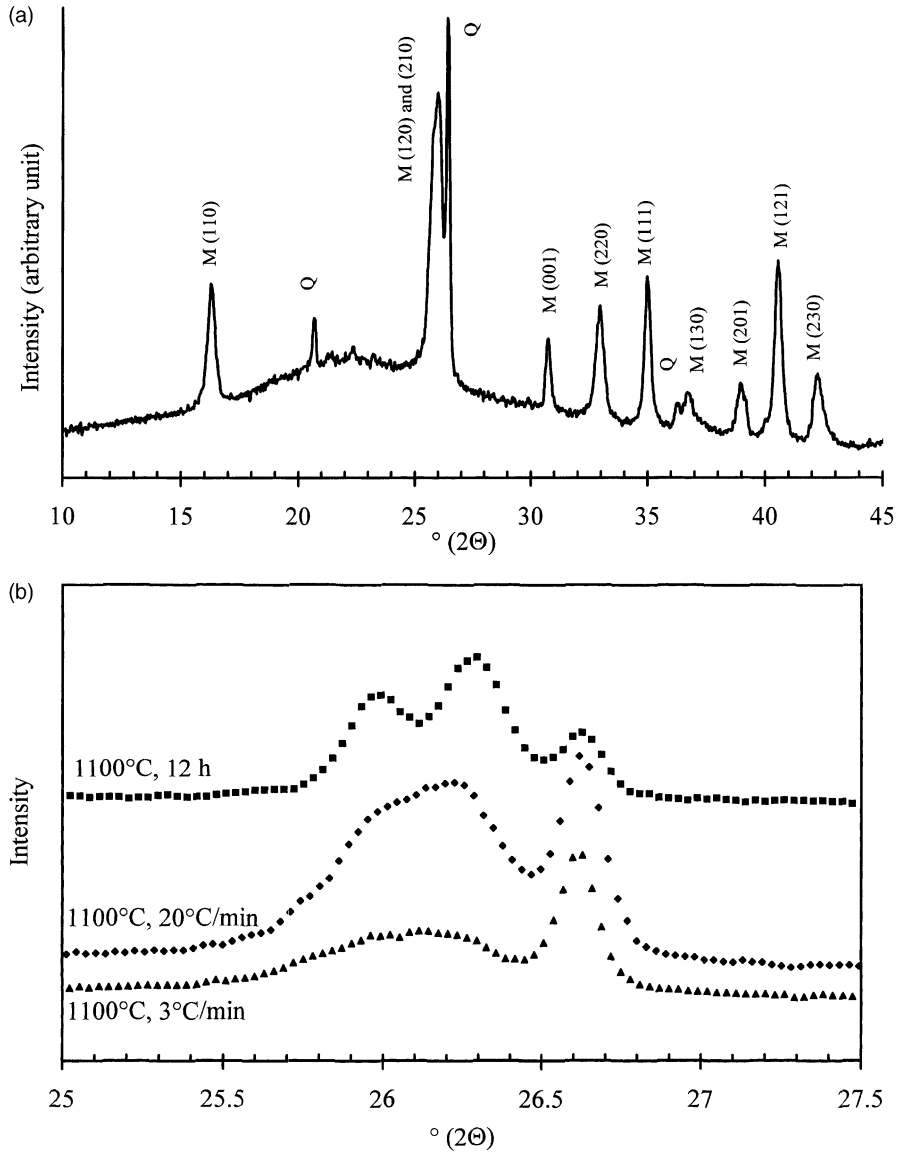

Fig. 1. (a) X-ray diffraction pattern of Bio kaolin sintered at 1100°C, 3°C/min; (b) detailed part of X-ray pattern for Bio kaolin for three thermal treatments.

reflection is close to 0.052 nm^{-1} and the corresponding value for the (00l) reflection is 0.022 nm^{-1}.

The crystallite sizes reported in Table 2, in relation to temperature and the temperature rate, show that mullite nano-crystals are always elongated along the c axis. The variations between values are significant when compared with measurement uncertainties.

Images from transmission electron microscopy of Bio fired at 1100°C, 3°C/min and 1150°C, 20°C/min are presented in Fig. 4a and b respectively. The presence of an amorphous phase containing small needle like crystallites was observed. The crystalline phase was always identified as mullite by micro-diffraction although there were various crystallographic orientations. Three examples are presented in Fig. 5. Additional observations by local microanalysis of potassium and iron elements indicated the following.

- Potassium is not present in mullite crystals or nearby. This strongly suggests that the amorphous phase results only from metakaolinite transformation, and not from the mica material produced by the high temperature.
- Iron-rich small zones were detected in the amorphous phase, but did not relate to the position of mullite crystals.

The lattice parameters of mullite were calculated from the peak positions using the least square fit procedure of "U. Fit" software.[14] The precise positioning of the sample was calculated using the peak position of an

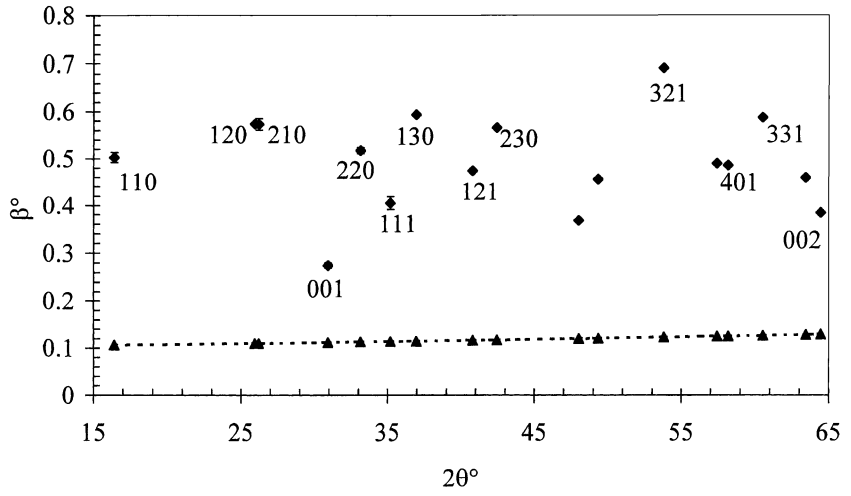

Fig. 2. Instrumental resolution function against 2θ, compared to various integral breadth of mullite reflections.

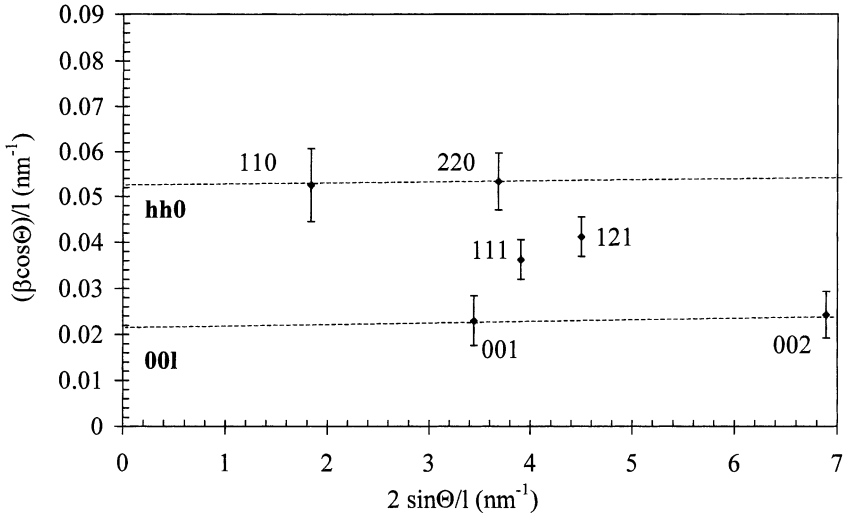

Fig. 3. Williamson and Hall plot of (hh0) and (00l) directions of mullite, for samples preliminary sintered at 1100°C, 3°C/min.

Table 2
Crystallite sizes of mullite from Bio kaolin, preliminary sintered at 1100°C, 3°C/min and 1150°C 20°C/min

	Temperature rate			
	3°C/min		20°C/min	
	(00l)	(hh0)	(00l)	(hh0)
Temperature (°C)	L (nm)	L (nm)	L (nm)	L (nm)
1100	26±4	16±2	50±10	21±3
1150	48±10	19±3	50±10	30±3

internal standard (silicon NIST, SRM 640a) mixed with the studied sample. The angular calibration of the position- sensitive detector was carried out according to the procedure previously described.[8] Results of a, b and c parameters and the lattice volumes are given in Table 3 against temperature and sintering rate.

4. Discussion

At the early stage of mullite crystallisation, without detectable liquid phase, the crystallite sizes along (00l) and (hk0) directions vary with thermal treatment (Table 2). All sizes increase as the temperature rises for both temperature rates. At a fixed temperature, however, the rise in the temperature leads to an increase in crystallite sizes. At 1150°C this increase is more accentuated. In particular at a temperature of 1150°C and at 20°C/min the anisotropic character of mullite crystallites decreases. A comparison with TEM observations (Fig. 4a and b) confirms the variation of the appearance relationship, although crystallite sizes are not representative.

A connection between mullite quantity and mullite crystallite sizes can be made using previous results[6] with the same kaolin material. These showed that, at the

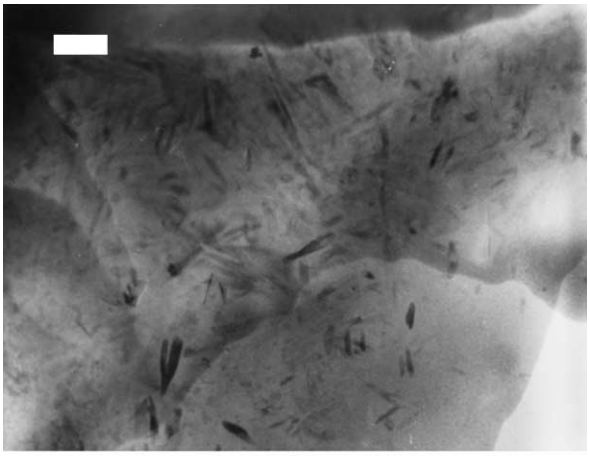

(a)

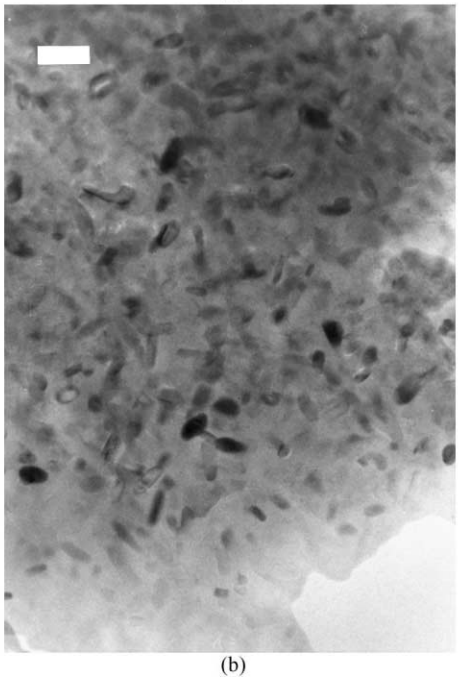

(b)

Fig. 4. (a) TEM image of mullite crystals in an amorphous material from Bio kaolin sintered at 1100°C, 3°C/min; (b) Bio sintered at 1150°C, 20°C/min. Bar = 100 nm.

1100°C intermediate temperature, mullite quantity increased from 4.2 to 10 wt.% when the sintering rate rose from 3 to 20°C/min. From sizes indicated in Table 2, therefore, which vary sharply, it is suggested that the increase of the temperature to 1100°C has more effect on the crystallite size rather than the crystallite number, i.e. the mullite growth mechanism.

Additional X-ray microanalysis indicated no correlation between potassium analyses and the mullite or the matrix phase. This shows that mullite needles are only found in the kaolinite-transformed phase. Consequently, the muscovite high temperature transformed phase behaves independently of neighbouring phases, up to 1150°C. Iron was analysed only in very small rich zones located in the amorphous phase matrix. Its presence is not surprising since a small part of iron in Bio is initially found as a structural element of the kaolinite mineral.[2] During heating, the important phase change in clay minerals leads to the formation of small clusters, mostly containing iron, which may be hematite.[15] Their distribution in the material has no correlation with that of mullite, which suggests that the role of iron in the mullite formation mechanism is very limited.

A linear correlation between the a mullite lattice parameter and the alumina content was found by Cameron,[16] especially for orthorhombic mullite. A more recent study from Okada[17] proposed a slightly different linear relation for both pseudo tetragonal and orthorhombic structures. The discrepancy between the two interpretations is more noticeable at high alumina content and is caused by a relative variation in the a and c axis for the pseudo tetragonal phase caused by some lattice disordering. The resulting length for the c axis for pseudo tetragonal mullite is smaller than that for orthorhombic mullite, in the case of two mullites having the same a axis.

In this study, the mullite alumina content was calculated on the basis of Cameron (Fig. 6a and b) linear relation, against the a lattice constant. The results were in a narrow range, about 62–65 Al_2O_3 %. Using the Okada correlation only slightly extended the alumina content to higher percentages. The standard deviation of Al_2O_3 content varies within the whole composition domain and is at about 1% for the range analysed.[16,17] A significant difference, therefore, was found between samples obtained at 3°C/min and 20°C/min, but not influenced by temperature. The corresponding b distances for all samples are also plotted in Fig. 6a. They are close to values published by Cameron and Okada. Since a lengths differ sharply from b lengths, this should be a preliminary indication of the orthorhombic character of mullite. Additional information is provided by c length values (Fig. 6b), which fit the Cameron relation satisfactorily. The relatively short c lengths further support the fact that orthorhombic mullite is always found in Bio, at 1100 and 1150°C. It must be emphasised that lattice parameters are always situated inside the orthorhombic mullite area presented by Okada for a large number of various mullites, (Fig. 3 in[17]).

Table 3 shows a comparison made with samples, which were first sintered at both temperatures and temperature rates, but maintained at these temperatures for 12 h. Results for *a*, *b* and *c* lattice parameters are given in Table 3 and plotted in Fig. 6. The *c* length appears to be slightly reduced, compared with the almost similar *c* lengths from materials sintered at 20°C/min. The very small variation from the above-mentioned results, compared with the measurement uncertainties, is not a precise indication of the stœchiometry variation and the modification of the orthorhombic character. Nevertheless, the clear splitting of the (120) and the (210) X-ray

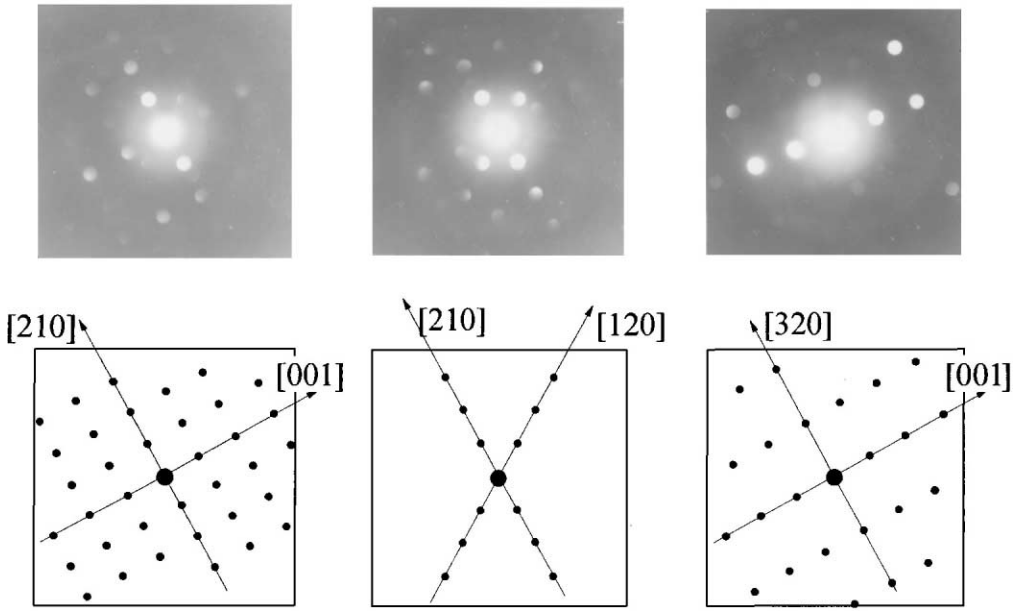

Fig. 5. Micro-diffraction analyses of mullite crystals along three different orientations.

Table 3
Lattice constants of mullite from Bio kaolin preliminary sintered at 1100 and1150°C for two temperature rates; 3°C/min and 20°C/min. The 3rd and 4th lines are from materials sinterted at 1100°C, 3°C/min and 20°C/min and maintained during 12 h

		a (Å)	*b* (Å)	*c* (Å)	Vol (Å^3)
3°C/min	1100°C	7.5537±0.0032	7.6976±0.0025	2.8858±0.0005	167.79
	1150°C	7.5560±0.0036	7.6937±0.0032	2.8859±0.0007	167.76
20°C/min	1100°C	7.5681±0.0042	7.7022±0.0032	2.8858±0.0007	168.21
	1150°C	7.5664±0.0015	7.7017±0.0014	2.8871±0.0004	168.24
3°C/min	1100°C, 12 h	7.5641±0.0029	7.7013±0.0017	2.8883±0.0008	168.25
20°C/min		7.5626±0.0029	7.7003±0.0018	2.8877±0.0005	168.16

reflection lines (Fig. 1b) supports this idea. In which case, there is no doubt that the very long sintering time encourages the presence of larger mullite crystals, reducing the X-ray line breadth. For samples sintered without any hold time, the apparent reflection overlap is mainly due to the very low crystallite size. The presence of an orthorhombic mullite should not therefore be dismissed.

A transition from pseudo tetragonal to orthorhombic mullite was reported in,[17,18] i.e. at about 1200°C and 62–63 Al_2O_3 %, for various sintered mullites. For the sintered Bio material, it was observed that orthorhombic mullite occurs with alumina content up to about 65% and at the 1100°C temperature.

In general, for kaolinite mineral, the formation routes of mullite are either a direct formation route or a transitory spinel phase formation before mullitisation, depending on the kaolinite phase and the thermal process.[19,20] At the lowest temperatures, poorly ordered nano-crystals nucleate from the disordered metakaolinite phase. They correspond to pseudo tetragonal mullite. At a higher temperature, the process is governed by the growth of more ordered mullite crystals. Their stochiometry is different because the growth stage implies a long-range diffusion between alumina-rich and silica-rich zones, which are segregated under the influence of temperature and time. This explains the stœchiometry difference between low and rapid thermal cycles of Bio, because the former one encourages silica enrichment. The presence of well-crystallised orthorhombic crystals in Bio indicates that mullite at the 1100°C temperature and above, for a 3 and 20°C/min temperature rate, is mainly transformed through a growth process. A similar trend is observed when comparing the cell volumes of rapidly sintered samples, which are almost equivalent, to cell volumes for 12 h sintered samples.

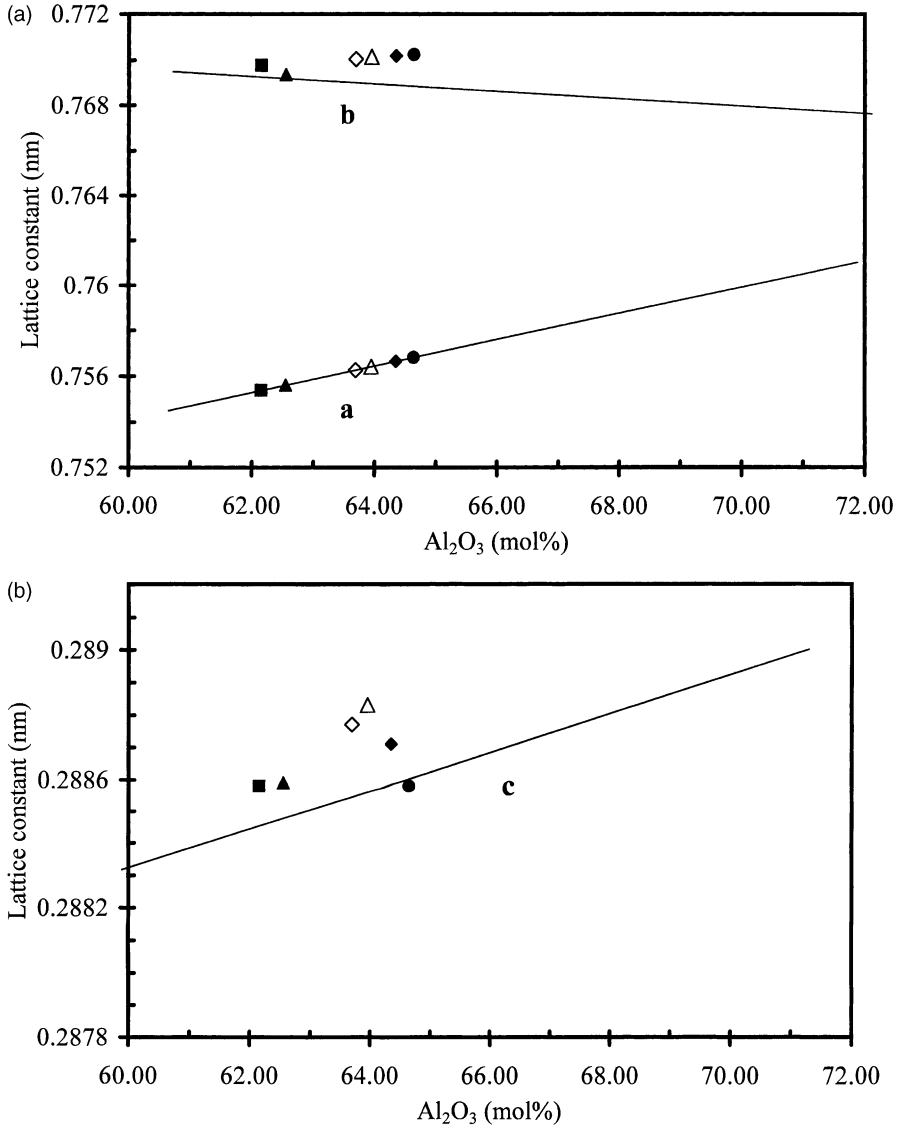

Fig. 6. Lattice constants and cell volumes of mullite versus the thermal cycle, compared to the average data from[17] (a) a and b constants; (b) c constant. (■): 1100°C, 3°C/min; (▲): 1150°C, 3°C/min; (●): 1100°C, 20°C/min; (◆): 1150°C, 20°C/min; (△): 1100°C, 3°C/min, 12 h; (◇): 1100°C, 3°C/min, 12 h.

5. Conclusion

Mullite formation was observed at the early stage of crystallisation, in the absence of liquid phase. Size and shape of crystals as the corresponding cell constants vary in relation to sintering temperature, but mainly in respect of the temperature rate. Using the Cameron relationship, it appears that mullite stochiometry remains in a narrow composition domain. At high temperatures rates, in particular, the mullite silicon content is reduced. At the very least, orthorhombic mullite was identified, in spite of a relatively low temperature between 1100 and 1150°C.

References

1. Castelein, O., Bonnet, J. P. and Blanchart, P., Comparison between high temperature behaviours of a kaolin raw material and reference minerals. *Annales de Chimie, Sciences des Matériaux*, 2000.
2. Castelein, O., *Influence de la vitesse du traitement thermique sur le comportement d'un kaolin: application au frittage rapide*. PHD thesis, Limoges University, 2000.
3. Baudson, H., Debucquoy, F., Huger, M., Gault, C. and Rigaud, M., Ultrasonic measurement of MgO/C refractories Young's modulus at high temperature. *Journal of the European Ceramic Society*, 1999, **19**, 1895–1901.
4. Osborn, E. F. and Muan A., Phase equilibrium diagrams of oxide systems, Plate 5. Am. Ceram. Soc., Jr. Ceram Fundation, 1960.
5. Baudet, G., Boulmier, J. L., Piantone, P. and Pillard, F. Caracteristiques geochimiques et mineralogiques des mineraux argileux affectant les proprietes rheologiques des kaolins d'Echassieres. Princ. Result. Sci. Tech.–Bur. Rech. Geol. Minieres, 1986, pp. 180–182
6. Castelein, O., Bonnet, J. P. and Blanchart, P., Influence of the heating rate on the thermal behaviour and mullite formation from a kaolin raw material. Accepted in *Ceramic International*, 2000.

7. Pruet, R. J. and Webb, H. L., Sampling and analysis of Kg1 well crystallized kaolin source clay. *Clay and Clay Minerals*, 1993, **41**, 514–519.
8. Masson, O., Guinebretière, R. and Dauger, A., Reflection Debye–Scherrer powder diffraction with flat plate sample using CPS 120 Inel: d-spacing accuracy and Rietveld refinement. *J. Appl. Crystallogr*., 1996, **29**, 540–546.
9. Masson, O., Guinebretière, R. and Dauger, A., Profil analysis in a symmetric powder diffraction with parallel beam geometry and curved position sensitive detector. *Material Science Forum*, 1998, **278-281**, 115–120.
10. Masson, O., Guinebretière, R. and Dauger, A. O. Modelling of line profil asymmetry caused by axial divergence in powder diffraction. Submitted to *J. Appl. Crystallogr*.
11. Langford, J. I., A rapid method for analysing the breadths of diffraction and spectral lines using the Voigt function. *J. Appl. Crystallogr*, 1978, **11**, 10–14.
12. Balzar, D., Voigt function model in diffraction line broadening analysis. In *Defect and Microstructure Analysis by Diffraction, IUCR Monograph on Crystallography No. 10*, ed. R.L. Snyder, J. Fiala and H.J. Burge. Oxford Sci. Publication, pp. 94–124.
13. Williamson, G. K. and Hall, W. H., X-ray lines broadening from file aluminium and wolfram. *Acta Metall*., 1953, **1**, 22–31.
14. Evain, M. U.Fit: a Cell Parameter Pefinement Program. Institut des matériaux de Nantes. Nantes, France, 1992
15. Murad, E. and Wagner, U., The thermal behaviour of an Fe-rich Illite. *Clay Minerals*, 1996, **31**, 45–62.
16. Cameron, W. E., Composition and cell dimensions of mullite. *Ceram. Bull*., 1977, **56**(11), 1003–1011.
17. Ban, T. and Okada, K., Stucture refinement of mullite by the Rietveld method for estimation of the chemical composition. *J. Am. Ceram. Soc*., 1992, **75**(1), 227–230.
18. Scheider, H. and Rymon-Lipinski, T., Occurence of pseudotetragonal mullite. *J. Am. Ceram. Soc*., 1988, **71**(3), 162–164.
19. Brown, I. W. M., MacKenzie, K. J. D., Bowden, M. E. and Meinhold, R. H., Outstanding problems in the kaolinite–mullite reaction sequence investigated by ^{29}Si and ^{27}Al solid state nuclear magnetic resonance: High-temperature transformations of metakaolinite. *J. Am. Ceram. Soc*., 1985, **68**(6), 298–301.
20. Gualtieri, A., Belloto, M., Artioli, G. and Clark, S. M., Kinetic of the kaolinite–mullite reaction sequence. Part II: mullite formation. *Phys. Chem. Minerals*, 1995, **22**, 215–222.